Numerical modelling of UHPC and TRC sandwich elements for building envelopes

Lorenzo Miccoli, Patrick Fontana
BAM Federal Institute for Materials Research and Testing, Berlin, Germany

Gabriel Johansson, Kamyab Zandi, Natalie Williams Portal, Urs Müller
CBI Swedish Cement and Concrete Research Institute, Borås, Sweden

Contact: lorenzo.miccoli@bam.de

Abstract

In this paper a modelling approach is presented to reproduce the mechanical behaviour of sandwich panels via finite element analysis. Two types of panels were investigated in this scope of work. The first sandwich element was a textile reinforced concrete (TRC) panel with cellular lightweight concrete insulation and the second configuration was an ultra-high performances concrete (UHPC) panel with aerated autoclaved concrete insulation. The goal was to obtain a reliable numerical strategy that represents a reasonable compromise in terms of sufficient accuracy of the element characteristics and the computational costs. The results show the possibility of describing the composite action in a full sandwich panel. The achieved modelling approach will later be used for the optimization of TRC and UHPC panels in terms of minimizing the thickness, identifying the number and location of connectors, as well as evaluating varying anchorage systems.

Keywords: sandwich elements, ultra-high performance concrete (UHPC), textile reinforced concrete (TRC), autoclaved aerated concrete (AAC), cellular lightweight concrete (CLC), finite element analysis (FEA).

1 Introduction

The awareness of the environmental impact of the building sector is increasing. Steel reinforced concrete is the most commonly used construction material and also a material with a high energy consumption and carbon footprint. Large environmental gains may arise if an alternative to steel reinforced concrete is developed. In this context, ultra-high performance concrete (UHPC) and textile reinforced concrete (TRC) are shown to be promising alternatives with advantages such as lower energy consumption and reduced environmental impact. Predictions suggest that UHPC and TRC sandwich elements for building envelopes could have other benefits such as an increased service life, optimized use of building area due to thinner elements, and minimized maintenance due to non-corrosive reinforcing materials. An adequate building envelope ensures the protection against moisture ingress, heat loss in winter, excessive heating in summer and noise. In this framework, two prototypes of façade elements were developed. UHPC and TRC in combination with autoclaved aerated concrete (AAC) or cellular lightweight concrete (CLC) are presented. The typologies are load-bearing for TRC elements and non-load-bearing for UHPC elements. They were both conceived to be used for new buildings and for renovation of existing buildings. The goal for all panel solutions is to minimise element thicknesses, without compromising their structural integrity and overall U-value. Prefabricated concrete sandwich panels (PCSP) have been extensively produced and used for structural applications for decades. Because of reduced thickness in UHPC and TRC panels, the structural design of such elements is a great challenge, and can be best assisted by advanced non-linear finite element (FE) analysis. These analyses can be used both to better understand the structural behaviour of a sandwich panel with a particular design, and also to further optimize a

given design. Therefore, it is important to have appropriate analysis methods for the structural design of UHPC and TRC panels using advanced FE analysis, which makes up the primary focal point of this study. The goal was to obtain a reliable numerical strategy that represents a reasonable compromise of sufficient accuracy of the element characteristics and the computational costs. The objectives were (1) to lay out a multi-level structural analysis approach for design and optimization of sandwich elements, and (2) to illustrate how the approach may be used for evaluation of a particular design. The achieved modelling approach will, in future, be used for the optimization of TRC and UHPC panels in terms of minimizing the thickness, identifying the number and location of connectors, as well as evaluating varying anchorage systems.

2 Façade element components

In this study two kinds of insulation materials were employed: AAC and CLC. AAC provides a low thermal conductivity in combination with mechanical properties which is adequate as an insulation layer in composite elements [1]. CLC constitutes an affordable and sustainable alternative providing both structural and insulation characteristics. Two typologies are proposed in this work. The first one is a three-layer full panel with a structural layer of TRC and CLC insulation, including 3D carbon fibre grid as reinforcement and specially designed metal connectors (Figure 1). Connectors to transfer pressure and suction to load-bearing inner panel and anchors to transfer vertical and horizontal loads to the load-bearing inner panel are made of glass fiber reinforced polymer (GFRP). The second one is a two layer half panel with a structural layer of UHPC and AAC or CLC insulation. The general idea is to realise the external UHPC shell as a box-shaped element. Due to the support from the edges of the box no shear forces are generated in the UHPC-AAC/CLC interface during transport and service life. Thus, no additional connectors are necessary, provided that the bond between UHPC and AAC/CLC is sufficiently high to prevent the detachment of the layers when the composite element is tilted after demoulding and during transport. Moreover, the edges form a frame and improve the stiffness of the box-shaped element, allowing the decrease of the thickness of the exterior UHPC layer. Anchors to transfer vertical and horizontal loads to the load-bearing structure are made of steel. More details are reported in [2]. Figure 2 gives an overview of the geometry of the panels. The design was based on load assumptions required by Eurocode 2 [3].

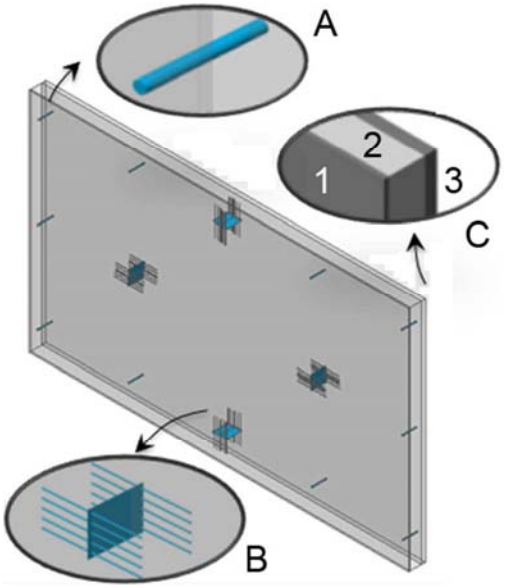

Figure 1. TRC full panel, load-bearing: 5 m × 3 m. GFRP pin-connector (A), GFRP flat anchor (B), TRC outer panel made of fine-grained concrete matrix + carbon textiles (C1), CLC insulation (C2), TRC inner panel (C2)

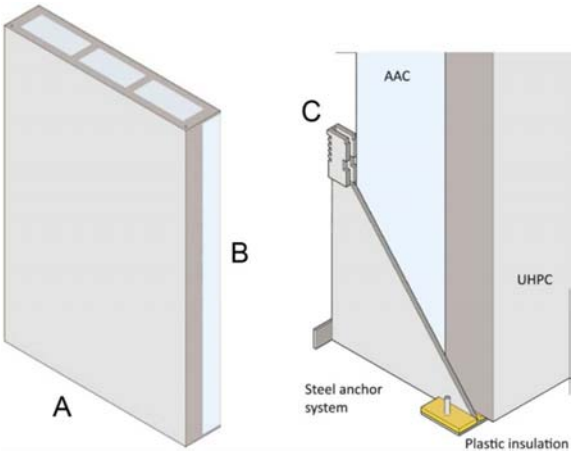

Figure 2. UHPC half panel, non-load-bearing: 2 m × 3 m. UHPC box-shaped element (A), AAC/CLC insulation (B), steel anchor (C)

2.1 Structural materials

2.1.1 TRC

Textile Reinforced Concrete (TRC) is a composite material fabricated of a fine-grained concrete matrix reinforced by bi- or multi-axial 2D and 3D textile fabrics. The replacement of conventional steel reinforcement with non-corrosive textile fibres could decrease the need for a thick concrete cover as it offers improved durability properties in concrete. These alternative reinforcement materials also offer a much lower density (1800-3000 kg/m^3) in comparison to steel reinforcement bars (7850 kg/m^3) which further contributes to a reduction in dead weight. A fine-grained concrete with a minimum aggregate size of d_{max} 4 mm was used. The exclusion of large aggregates increases shrinkage which introduces substantially more internal microcracks. The defects inherently cause the tensile strength of the matrix to reduce. Considering these aspects a tensile strength in the order of about 4% of the compressive strength was adopted (Table 1).

2.1.2 UHPC

UHPC exhibits extreme high strength and excellent chemical durability. The exceptional properties of UHPC are the result of a high packing density based on an optimised particle size distribution and significant reduction of water in the cement paste compared to ordinary concrete [4]. The UHPC adopted is based on Dyckerhoff Nanodur® technology. Nanodur compound contains ultrafine components (Portland cement, blast furnace slag, quartz, synthetic silica) smaller than 250 µm that are dry mixed intensively. Further reduction of embodied energy was achieved by the replacement of Portland cement with less energy intensive types of cement or supplementary cementitious materials (SCM) originating also from industrial residuals.

2.2 Insulation materials

2.2.1 AAC

The material structure of AAC is characterised by a solid skeleton and aeration pores being formed during the aluminum-driven expansion of the slurry. The foam-like structure of AAC, with its solid skeleton acting as partitioning walls between the aeration pores [5], leads to an optimum correlation between weight and compressive strength. Millions of aeration pores lead to a low thermal conductivity making AAC a highly thermal insulating building material. Thermal conductivity depends on temperature, density, structure and chemical nature of the material. For this reason, improvements of the thermal performance of AAC had been mainly achieved by reducing the dry density.

2.2.2 CLC

In order to be used as a high performance insulation material, very low density CLC was developed. Given the high volume of foam, the main challenge is to guarantee that the cementitious matrix sets fast enough to sustain the porous structure without collapse of the foam. For this purpose, calcium aluminate cement was chosen as binder, which sets much faster when compared to Portland cement. In CLC, the mechanical properties are very much dependent on the homogeneity of the air void distribution.

3 Multi-level structural modeling

The multi-level structural analysis of sandwich panels in this paper is based on the multi-level structural assessment strategy for reinforced concrete bridge deck slabs proposed in Plos *et al.* [6] with the principle of successively improved evaluation in structural analysis outlined in Sustainable Bridges [7][8]. Both structural elements, slabs and panels, share some similarities in terms of structural behaviour, and thus could be modelled in FEA following the same principals. In Figure 3, a flow diagram for the analyses is illustrated. It starts with an initial design using simplified analysis methods. However, for an in-depth evaluation of a design as well as optimization of a design, more advanced structural analyses describing all possible failure modes and resistance models that are more accurate and reliable are needed. Some of these analyses are described below in detail.

3.1 3D linear shell analysis

Here, the structural analysis is performed using 3D FE models, primarily based on shell or bending plate theory. The analysis is made assuming linear response to be able to superimpose the effect of different loads, in order to achieve the maximum load effects in terms of cross-sectional forces and moments throughout the structure for all possible load combinations. Since both geometrical simplifications and the assumption of linear material response result in unrealistic stress concentrations, and because the rebar are normally arranged in strips with equal bar diameter and spacing, the redistribution of the linear cross-sectional forces and moments are necessary. Recommendations on redistribution widths for bending moments and shear forces are given in Pacoste et al. [9]. The structural analysis can be seen as "linear elastic with limited redistribution" according to Eurocode 2 [3]. The load effect is then compared with corresponding resistance in similar way as at level I.

3.2 3D non-linear shell analysis

In a non-linear analysis, the loads are successively increased until failure of the structure is reached. In practice, due to the excessive amount of work it would require, non-linear analysis cannot be made for all possible load combinations, but only for the most critical loads. At this level, shell (or bending plate) finite elements are used. The reinforcement is included in the FE model but assumed to have perfect bond to the concrete; it is preferably modelled as embedded reinforcement layers in the shell elements, strengthening the concrete in the direction and at the level of the reinforcement bars. In such a model, bending failures will be reflected in the analysis, whereas out-of-plane shear, punching, or anchorage failures are not reflected. Instead they must be checked by local resistance models. With this level of accuracy on the structural analysis, resistance models at higher levels of approximation according to MC2010 [10] are preferably used. For shear type failures, models taking into account the in-plane stress-state from the non-linear analysis are recommended.

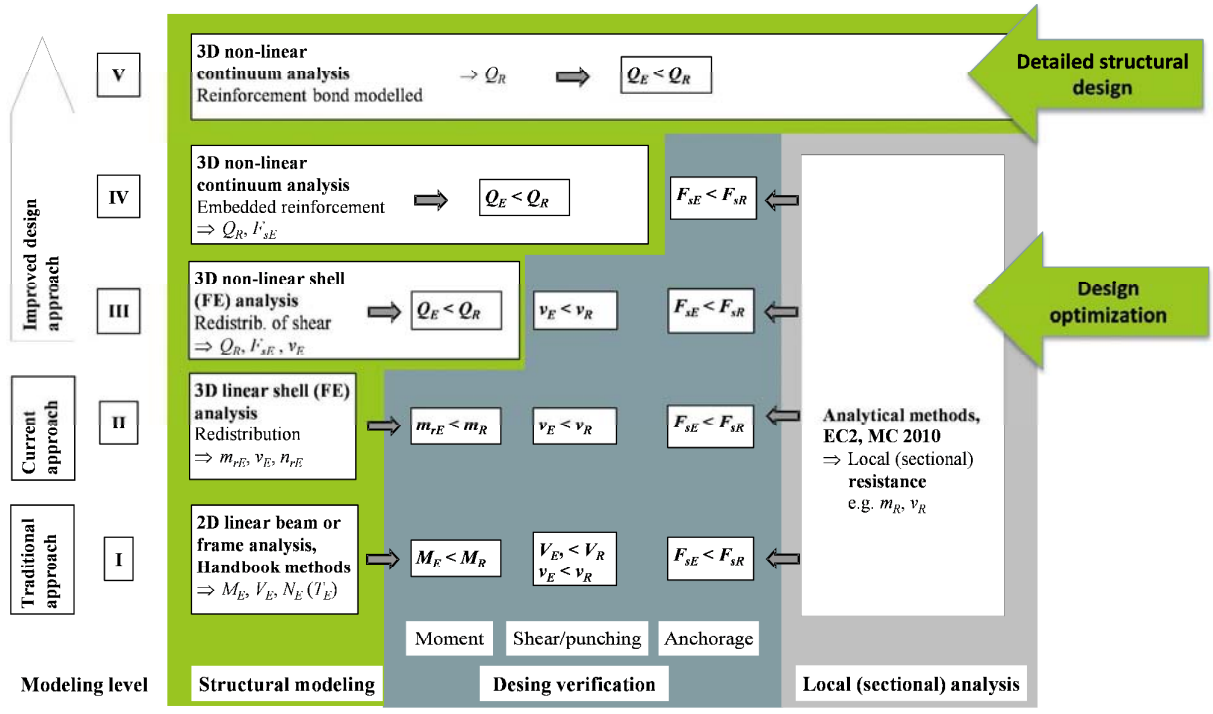

Figure 3. Scheme for multi-level structural modelling of RC element, adopted from Plos et al. (2015)

3.3 3D non-linear continuum analysis

Compared to the level IV analysis, the reinforcement is modelled using separate finite elements. Furthermore, the bond-slip behaviour of the interface between the reinforcement and the concrete is included.

With a fine mesh, individual cracks can be studied and anchorage failure can be reflected in the analysis. With this level of accuracy in the structural analysis, the intention is that no major failure modes should be necessary to check using separate resistance models.

3.4 Modelling the effect of deterioration

When the structure is deteriorated due to reinforcement corrosion, frost damage or alkali-silica reaction, the structural effect of the deterioration needs to be accounted for in the analysis. At levels I and II, the deterioration will affect the structural analysis only if the stiffness relations are altered, whereas the resistance calculations are more directly influenced. With non-linear structural analysis at levels III – V, lowered material strengths, concrete cover spalling and deteriorated reinforcement-concrete interactions may be directly included in the FE model. Recommendations on how to take into account the effect of deterioration can be found in Zandi et al. [12] for corrosion and in Zandi et al. [11] for frost. No deterioration however is included in the analyses presented in this paper.

3.5 Safety format

For each level of analysis, a relevant safety format should be used. When a two-step procedure is used to determine the load-carrying capacity, as at levels I and II, the partial factor method is normally used. For non-linear analysis, using a one-step procedure to determine the load-carrying capacity at the structural level, safety formats based on global safety factors according to MC2010 [10] are recommended. This applies to level V as well as levels III and IV for the types of failures reflected in the non-linear analysis. When there are failure modes which are not reflected in the analysis, these are checked using separate resistance models, such as the partial factor method. When safety formats based on global safety factors are used, and bending failures in skew directions and shear type failures govern the capacity, the modelling uncertainty used should be given special attention. For the case studies below, the different analysis levels are compared using mean values. In this way, the variance safety formats do not influence the comparison. Instead, it is the ability of the structural analysis and resistance models to predict the load-carrying capacities that is evaluated.

4 Modelling of TRC panel at level V

4.1 FE mesh

Given the symmetry lines, only a quarter of the TRC panel was included in the FE model. Nodal translations were prevented in x-direction along symmetry line 1, in z-direction along symmetry line 2, and in y-direction along the edge of the inner panel. Concrete, insulation and connectors are all modelled with 3D solid elements which are based on numerical integration with 1-point integration scheme over the volume. The mean element size was 10 mm. The textile reinforcement is modelled as grid reinforcement, embedded in solid elements with prescribed bond-slip relation (Figure 4).

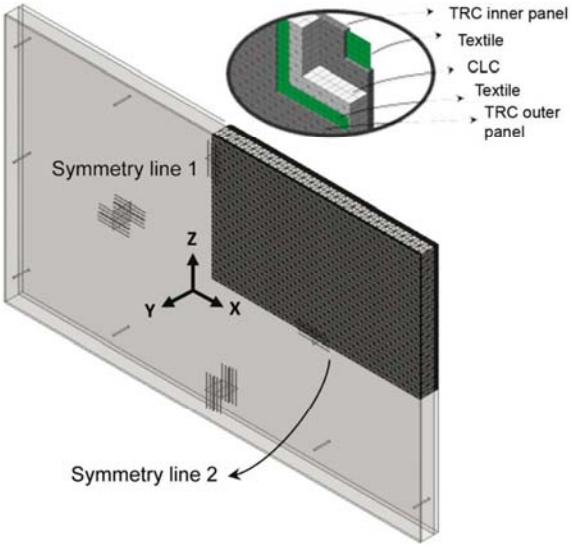

Figure 4. TRC full panel numerical modelling

4.2 Material properties

For the compressive behaviour of the concrete, a modified Thorenfeldt curve was used. The original Thorenfeldt curve describes the stress-strain relationship of a 300 mm long cylindered concrete specimen. As the strain values in the curve are dependent on the specimen length, the strain needs to be modified to the length of the crushing elements in the model according to [12]. It is assumed that crushing occurs in one element row above or below the embedded connectors (which was later verified in the analysis) and therefore the Thorenfeldt curve is modified to the appropriate size of 10 mm. For tensile behaviour of the concrete, the tension softening was taken into account using a predefined Hordijk´s curve in DIANA. The material properties adopted are reported in Table 1.

Table 1. Material properties for TRC panel

Concrete	Compressive strength [MPa]	84.7
	Tensile strength [MPa]	3.1
	Young´s modulus [GPa]	41.8
	Fracture energy [N/m]	146.2
Insulation	**Linear elastic material properties**	
	Young´s modulus [GPa]	15
	Poisson's ratio [-]	0.2
Textile	**Linear elastic material properties**	
	Young´s modulus [GPa]	230
	Poisson's ratio [-]	0.2

4.3 Analysis procedure

The crack model chosen for the concrete was a total strain based model with rotating crack approach. The effective bandwidth length was assumed to match the element sizes. Three analyses were carried out using different loading sets which are described in section 4.4. An incremental static analysis was made using an explicitly specified load step size and a Newton–Raphson iterative scheme to solve the non-linear equilibrium equations.

4.4 Results

Three analyses were carried out using different loading sets; the results in term of load-deflection curves are shown in Figures 5 and 6. In the first analysis, the imposed load was applied as a distributed load on the top of the inner panel; see Figure 5. The maximum imposed load at the ultimate limit state (ULS) for a 3m x 5m panel located in the ground floor of a 5-storey building was calculated to be 255 kN/m; this is marked "ULS" in Figure 5. The analysis showed that the panel can resist an imposed load well above the ULS load. The panel ultimately failed at the load level of approx. 400 kN/m due to crushing of the inner panel at the loading position. This indicates that higher loads can be carried if the loading area of the inner panel could be increased.

In the second analysis, the compressive strength of concrete at the top of the inner panel was increased by 30%, which hypothetically would have the same impact as if the loading area had been increased. Moreover, panel warping caused by shrinkage and unfavourable temperature gradient of 20 °C was included prior to impose loading. The results shown in Figure 5 illustrate that a total deflection of 2.71 mm at the middle of the panel has taken place due to shrinkage and temperature loads prior to imposed load, and that increased concrete strength have led to increased load-carrying capacity of the panel. It should be noted that in both analyses the stresses in the textile reinforcement have been relatively small and that no indication of bucking in the panel was observed.

In the third analysis, the loads were applied in the following order: (a) shrinkage load, (b) temperature gradient of 20 °C, (c) ULS imposed load of 255 kN/m, and (d) wind load as a pressure on the surface of the outer panel up to the failure of the panel. The maximum wind load at ULS for a panel located in the top floor of a 5-storey building in Stockholm region was calculated to be -1.41 kN/m^2; this is marked "ULS" in Figure 6. The analysis has shown relatively small stresses in pin connectors but high stresses in the concrete around the pin connectors. The preliminary failure was found to be the failure of outer panel in bending, and a final failure mode was the

anchorage failure of textile reinforcement. Overall, the load-carrying capacity of the panel was higher than the ULS wind load.

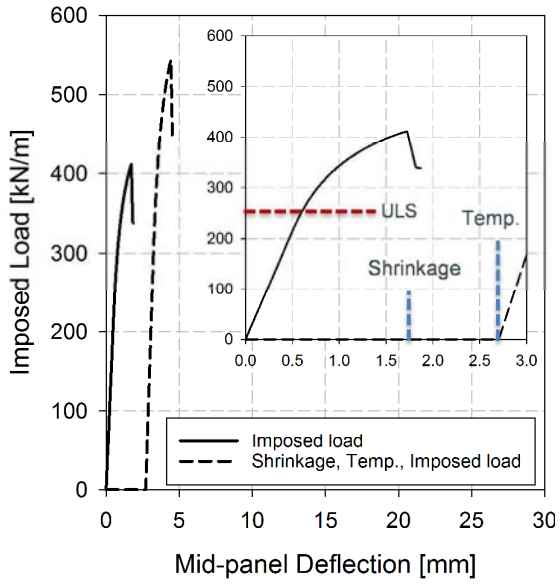

Figure 5. TRC full panel. Imposed load-mid-panel deflection curves

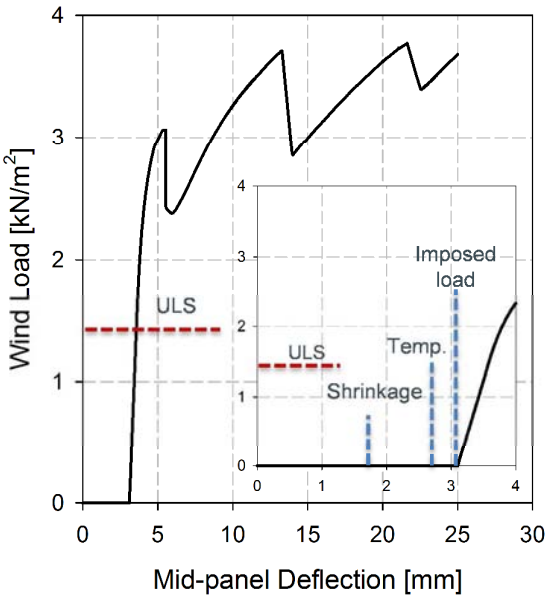

Figure 6. TRC full panel. Wind load-mid-panel deflection curves

5 Modelling of UHPC panel at level V

5.1 FE mesh

Similar to the TRC panel, only a quarter of the panel was included in the FE model. Nodal translations were prevented in x-direction along symmetry line 1, in z-direction along symmetry line 2, and in y-direction along the edge of the panel. Concrete, insulation and pin connectors are modelled with 3D solid elements which are based on numerical integration with 1-point integration scheme over the volume. The mean element size was 50 mm (Figure 7).

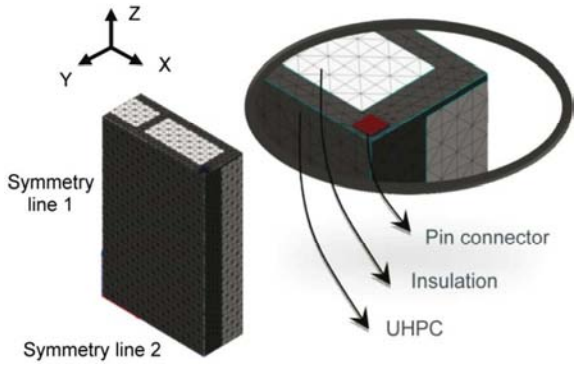

Figure 7. UHPC half panel numerical modelling

5.2 Material properties

The material data used for the modelling were mostly retrieved from experimental studies carried out. For the compressive and tensile behaviour of the concrete, the material properties below were used (Table 2). A linear elastic behaviour was assumed for the insulation.

Table 2. Material properties for UHPC panel.

UHPC	Compressive strength [MPa]	150.0
	Tensile strength [MPa]	15.0
	Young´s modulus [GPa]	60
	Fracture energy [N/m]	180
Insulation	**Linear elastic material properties**	
	Young´s modulus [GPa]	1.6
	Poisson's ratio [-]	0.2

5.3 Analysis procedure

The crack model chosen for the concrete was a total strain based model with rotating crack orientation. The effective bandwidth length was assumed to match the element sizes. Only the wind load was applied as a pressure on the surface of the outer panel. An incremental static analysis was made using an explicitly specified load step size and a Newton– Raphson iterative scheme to solve the non-linear equilibrium equations.

5.4 Results

The deflection curve obtained from the analysis is given in Figure 8. In general, three regions can be recognized in load-deflection curve that are marked on the figure and described below:

1) Region ①: bending cracks at the center of the panel appear one after the other.

2) Region ②: first the edge of the box gradually cracks and thus the additional stiffness from insulation material comes fully to play. Later, one major crack at the edge of the box leads to a sharp drop in the load.

4) Region③: cracks around the pin connectors take place and limit the capacity.

Overall, the load-carrying capacity of the panel was higher than the ULS wind load.

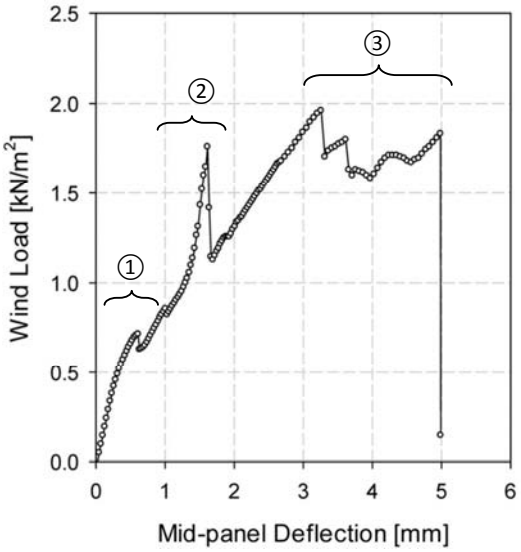

Figure 8. UHPC half panel. Wind load-mid-panel deflection curves

6 Conclusions

The goal of this paper was to obtain a reliable numerical strategy representing a reasonable compromise in terms of sufficient accuracy of the element characteristics and the computational costs. The possibility of describing the composite actions in load-bearing panels (TRC) and non-load-bearing panels (UHPC) was investigated. This work represents a preliminary study in which the capability of the structural analysis and resistance models to predict the load-carrying capacities is evaluated. A multi-level structural analysis of sandwich panels was first outlined. To reduce computational costs for both panel typologies only a quarter of the panel was included in the FE model. The thickness of structural layers for both sandwich panels was calibrated for a wind load of 1.7 KN/m^2. The analyses curves related to the wind load actions show a good correlation with the expected results in terms of design loads. The TRC panels show an out of plane resistance going over the design threshold. Following the load-displacement curve the first crack appear in correspondence of a wind load of about 3 KN/m^2. This result can be related to the beneficial effect of the multilayered section able to increase the global stiffness of the sandwich panel. For the UHPC panel the first crack appears in correspondence of a wind load of about 0.7 KN/m^2, confirming the low contribution of the insulation material to the global stiffness of the element.

7 Acknowledgments

This research study was made possible with the support of the European Union's 7th Framework Programme for research, technological development and demonstration under grant agreement no. 608893 (H-House, www.h-house-project.eu).

8 References

[1] *European Technical Approval ETA-05/0093. Multipor thermal insulation panel*. Valid to June 1st, 2019. 2011.

[2] Miccoli L., Fontana P., Silva N., Klinge A., Cederqvist C., Kreft O., Qvaeschning D., and

Sjöström C. Composite UHPC-AAC/CLC façade elements with modified interior plaster for new buildings and refurbishment. Materials and production technology. *Journal of Facade Design and Engineering*. 2015; **3**(1): 91-102.

[3] EN 1992-1-1. *Eurocode 2: design of concrete structures - part 1-1: general rules and rules for buildings*. Brussels, Belgium: CEN European Committee for Standardization. 2004.

[4] De Larrard F., and Sedran T. Optimization of ultra-high-performance concrete by the use of a packing model. *Cement and Concrete Research*. 1994; **24**: 997-1009.

[5] Alexanderson, J. Relations between structure and mechanical properties of autoclaved aerated concrete. *Cement and Concrete Research*. 1979; **9**(4): 507-514.

[6] Plos M., Shu J., Zandi K., and Lundgren K. A multi-level structural assessment proposal for reinforced concrete bridge deck slabs. *Structure and Infrastructure Engineering*. 2015 (submitted).

[7] *Sustainable bridges. Guideline for load and resistance assessment of existing European railway bridges: advices on the use of advanced methods*. 2007.

[8] Sustainable bridges. Non-linear analysis and remaining fatigue life of reinforced concrete bridges. 2007.

[9] Pacoste C., Plos M., and Johansson M. *Recommendations for finite element analysis for the design of reinforced concrete slabs*. Stockholm: TRITA-BKN Rapport 114. 2012.

[10] CEB-FIP. *Fib model code for concrete structures*. Lausanne: 2013.

[11] Zandi Hanjari K., Kettil P., and Lundgren K. Modelling the structural behavior of frost-damaged reinforced concrete structures. *Structure and Infrastructure Engineering*. 2010; **9**(5): 416–431.

[12] Zandi Hanjari K., Kettil P., and Lundgren K. Analysis of mechanical behavior of corroded reinforced concrete structures. *ACI Structural Journal*. 2011; **108**(108): 532–541.